PHYSICAL REVIEW B **89**, 241201(R) (2014)

Ohmic current in organic metal-insulator-metal diodes revisited

G. A. H. Wetzelaer[1] and P. W. M. Blom[2]

[1]*Zernike Institute for Advanced Materials, University of Groningen, Nijenborgh 4, 9747 AG Groningen, The Netherlands*

[2]*Max Planck Institute for Polymer Research, Ackermannweg 10, 55128 Mainz, Germany*

(Received 27 November 2013; revised manuscript received 5 February 2014; published 27 June 2014)

In the classical analysis of charge transport in solids by Lampert in 1956 an Ohmic current is attributed to the presence of a background carrier density due to (unintentional) doping. We demonstrate that Ohmic currents are also observed in undoped semiconductors as a result of diffusion of charge carriers from the contacts into the semiconductor. This Ohmic diffusion current shows an enhanced thickness scaling and is governed by the charge-carrier mobility. Specific for organic semiconductors the charge-carrier density dependence of the mobility at zero electric field can be accurately determined from the Ohmic diffusion current.

DOI: 10.1103/PhysRevB.89.241201 PACS number(s): 72.80.Le, 72.80.Ng, 73.40.Rw, 73.40.Sx

A widely used method to characterize charge transport in undoped solids is by measuring space-charge-limited currents [1,2]. When an undoped semiconductor is sandwiched between two metallic electrodes, effectively a metal-insulator-metal (MIM) stack is formed. If the injecting electrode forms an Ohmic contact, i.e., there is no injection barrier, and the collecting electrode has a sufficiently large barrier to prevent injection of charge carriers of the opposite sign, the current in the device is due to one type of carrier only. The current in such a single-carrier device will be limited by the buildup of uncompensated charges in the layer, giving rise to a space-charge-limited current. The well-known expression for the space-charge-limited current (SCLC) in a MIM device has been obtained by Mott and Gurney in 1940, given by [1]

$$J = \frac{9}{8}\varepsilon\mu\frac{V^2}{L^3}, \tag{1}$$

with J the current density, ε the permittivity, μ the charge-carrier mobility, V the voltage, and L the layer thickness. A built-in voltage V_{bi} exists when electrodes with different work functions are used. In that case, the alignment of the Fermi levels of the electrodes in thermal equilibrium will result in a built-in electric field across the insulator or semiconductor layer. At voltages below the built-in voltage, the electric field points in the opposite direction of the current, implying that the drift current is negative and that the current is dominated by diffusion of charge carriers [3]. Above the built-in voltage, the electric field and current point in the same direction, giving rise to a SCL drift current. In this case Eq. (1) can still be applied by replacing V by an effective voltage $V - V_{\mathrm{bi}}$, such that the mobility can be extracted directly from current-voltage characteristics of a single-carrier MIM device.

In the case that there are already thermal free carriers with density p_0 available in the semiconductor due to (unintentional) doping, at low voltages the current will follow Ohm's law given by [4]

$$J = q\mu p_0\frac{V}{L}. \tag{2}$$

In this low-voltage regime the background density p_0 dominates over the injected excess carriers, whereas at a voltage of $8/9(qp_0L^2/\varepsilon)$ a transition to the quadratic SCLC occurs [4]. With the mobility known from the SCLC regime [Eq. (1)] the background carrier density is then directly obtained from the Ohmic regime [Eq. (2)]. A typical example of such a behavior is shown in Fig. 1 for a *symmetric* MIM diode based on the undoped organic semiconductor poly[2-methoxy-5-(2′-ethylhexyloxy)-*p*-phenylenevinylene] (MEH-PPV) with a layer thickness of 100 nm, sandwiched between poly(3,4-ethylenedioxythiophene): poly(styrenesulfonate) (PEDOT:PSS) and MoO_3/Al contacts. The work functions of PEDOT:PSS (∼5.2 eV) and MoO_3 (∼6.9 eV [5]) are sufficient to provide Ohmic hole injection into the MEH-PPV highest occupied molecular orbital of ∼5.3 eV below the vacuum level. As expected for two Ohmic contacts, the MEH-PPV devices fabricated in this study indeed show perfectly symmetric current-voltage characteristics (see Supplemental Material [6]), and a built-in voltage is absent. The *J*-*V* characteristics show an Ohmic current at low voltages and a transition to a quadratic voltage dependence at higher voltages. At low temperatures the *J*-*V* characteristics exhibit an even steeper slope, which is due to an electric-field and carrier-density dependent mobility [7].

Following the classical analysis, the mobility is extracted from the quadratic part (solid lines), and the background density from the linear regime (dashed lines). The extracted mobilities and densities are summarized in Table I. From the temperature dependence of p_0, a 40 meV activation energy for the doping process can be extracted. This analysis is straightforward and seems correct, but a major problem arises when the thickness dependence is considered, as shown in Fig. 2. For a fixed background carrier density, Eq. (2) predicts an Ohmic current which depends on the inverse of the layer thickness.

From Fig. 2 it is immediately clear that both the linear and quadratic regions have the same layer-thickness dependence. This becomes even more apparent when scaling the graphs as done in Fig. 2(b), where the product of the current density and the layer thickness is shown versus voltage. For a fixed p_0, the curves should be on top of each other in the linear regime. Clearly, this is not the case. It appears that both the linear and quadratic current regimes have much stronger thickness dependence. When multiplying the current density with L^3, the scaling is more accurate, as can be seen in Fig. 2(c). A $1/L^3$ thickness dependence is expected for space-charge-limited currents, but is not typical for Ohmic currents.

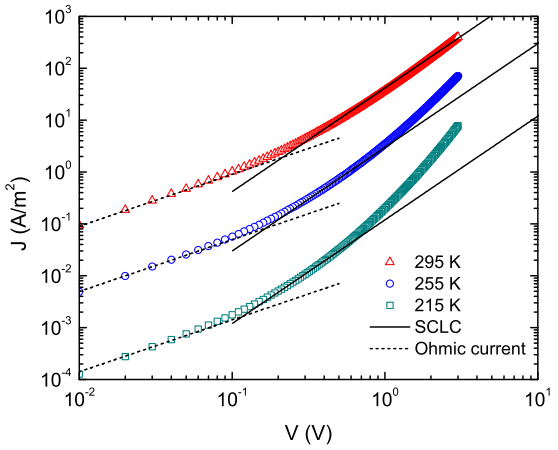

FIG. 1. (Color online) Temperature-dependent J-V characteristics of a symmetric MEH-PPV (100 nm) device. The dashed and solid lines represent fits with Eqs. (2) and (1), respectively.

In order to explain the thickness dependence of the observed Ohmic currents, the origin of the linear regime has to be investigated further. It is important to note that the classical analysis for the space-charge-limited current neglects diffusion; Eqs. (1) and (2) only take the drift contribution to the current into account.

In a recent study [3], we investigated the J-V characteristics in *asymmetric* MIM diodes with one Ohmic and one non-Ohmic contact, such that a built-in voltage $V_{\rm bi}$ is present. The diffusion-limited current in a MIM with an Ohmic contact on one side and a contact with injection barrier $\varphi_{\rm b}$ on the other side is described by [3]

$$J = \frac{q\mu N_v(\varphi_{\rm b} - b - V)\left[\exp\left(\frac{qV}{kT}\right) - 1\right]}{L\,\exp\left(\frac{qb}{kT}\right)\left[\exp\left(\frac{q(\varphi_{\rm b}-b)}{kT}\right) - \exp\left(\frac{qV}{kT}\right)\right]}. \tag{3}$$

The built-in voltage for a diode with asymmetric contacts is then given by $V_{\rm bi} = \varphi_{\rm b} - b$, which is the barrier at the collecting contact minus a reduction due to band bending as a result of accumulated charge carriers at the Ohmic injecting contact. The band-bending parameter b is given by [3,8]

$$b = \frac{kT}{q}\left[\ln\left(\frac{q^2 N_v L^2}{2kT\varepsilon}\right) - 2\right]. \tag{4}$$

At $V_{\rm bi}$ the current undergoes a transition from an exponential to a linear Ohmic dependence on voltage. Due to the thickness dependence of the band-bending parameter, the Ohmic current above $V_{\rm bi}$ depends inversely on L^3, similar to what is observed in Fig. 2 for the Ohmic regime of the symmetric MIM devices.

TABLE I. Mobility and background carrier density extracted with Eqs. (1) and (2), respectively, for a 100 nm MEH-PPV device.

T (K)	μ (m^2/V s)	p_0 (m^{-3})
295	1.4×10^{-9}	4×10^{21}
255	1×10^{-10}	3.1×10^{21}
215	4×10^{-12}	2.2×10^{21}

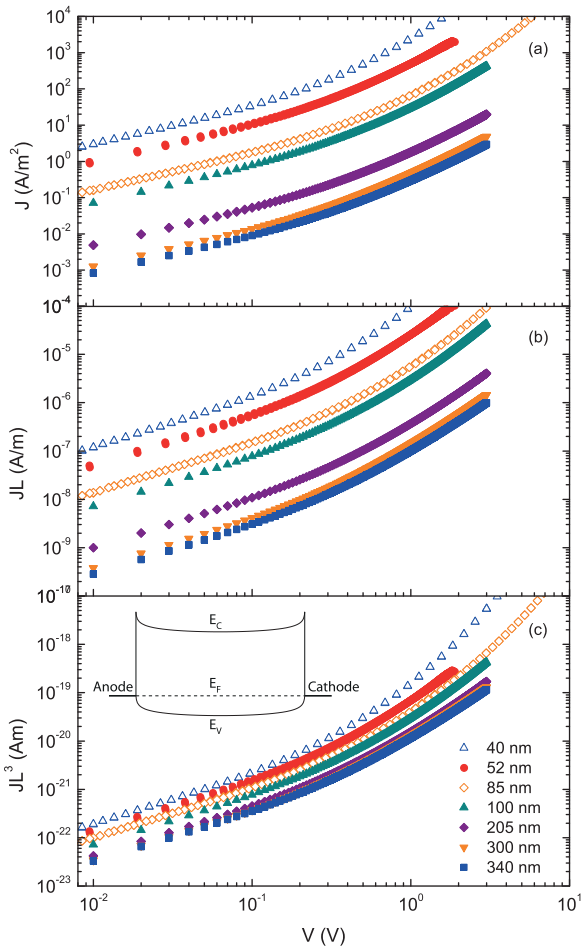

FIG. 2. (Color online) (a) J-V characteristics of symmetric MEH-PPV devices of different layer thicknesses at 295 K. Open symbols represent data from symmetric Au/MEH-PPV/PEDOT:PSS devices (see Supplemental Material [6]). The current density is multiplied by L (b) and L^3 (c), to show the layer-thickness dependence of the current. The inset shows a schematic band diagram of the device.

The diffusion current in a MIM device with two Ohmic contacts can be considered as a limiting case of the more general description given by Eqs. (3) and (4). Since a built-in voltage is absent in a symmetric MIM device, the diffusion current will always be in the linear regime, leading to a linear total current as long as the charges due to diffusion from the contacts exceed the injected excess carriers under bias. However, for a symmetric hole-only device with two Ohmic hole contacts, band bending due to diffused charges from the contacts occurs at both sides of the device, as schematically shown in the inset in Fig. 2. By setting $\varphi_{\rm b} = b$, this condition reduces Eq. (3) to an Ohmic current, according to

$$J = q\mu N_v \exp\left(-\frac{qb}{kT}\right)\frac{V}{L}, \tag{5}$$

which scales linearly with the charge-carrier mobility. Note that the $N_v\ \exp(-b/kT)$ term can be interpreted as an effective density of accumulated charge carriers p_0. Since in a symmetric device the charge-accumulation regions from the contacts overlap, the band bending in the device is slightly

reduced as compared to the case of one Ohmic contact [8]. In the center of the device, the charge concentration reaches its minimum value and so does the valence-band edge. The valence-band edge halfway across the layer, with respect to the equilibrium Fermi level, is given by [8]

$$E_v(L/2) = -kT \ln\left(\frac{q^2 N_v L^2}{2\pi^2 kT\varepsilon}\right), \tag{6}$$

which can be used to obtain the effective density of accumulated charge carriers (see Supplemental Material [6])

$$p_0 = \frac{4\pi^2 kT\varepsilon}{q^2 L^2}, \tag{7}$$

and a corresponding reduced band-bending parameter b' for a symmetric device given by

$$b' = \frac{kT}{q} \ln\left(\frac{q^2 N_v L^2}{4\pi^2 kT\varepsilon}\right). \tag{8}$$

The band-bending parameter b' according to Eq. (8) is observed to be about kT/q smaller than the band-bending parameter for an asymmetric device, Eq. (4). The reduction in band bending is also clear from Fig. 3 where it can be observed that the edge of the valence band halfway across the layer is higher for the symmetric case than for the asymmetric case. In Fig. 3(b) a graphical representation for b' is given; the band diagram including band bending (solid line) can be approximated by a flat band (dotted line) where b' represents the distance from the band edge to the Fermi level ($E_v = 0$) such that the density in the semiconductor is everywhere p_0. The effective injection barrier φ_b is then equal to b', leading to $V_{bi} = 0$ V. Finally, substituting b' [Eq. (8)] into Eq. (5) leads to a simplified expression for the Ohmic diffusion current,

$$J = 4\pi^2 \frac{kT}{q} \varepsilon\mu \frac{V}{L^3}. \tag{9}$$

An alternative method to obtain this result is to calculate p_0 from the density distribution $p(x)$ [9], yielding the same result for the current [10]. Here we show that the Ohmic current in a symmetric device is a special case of the general description of the diffusion current [Eq. (3)].

The experimental results in Fig. 2 for symmetric MEH-PPV hole-only devices indeed show that the layer-thickness dependence of the Ohmic part of the characteristics is better described when it is treated as a diffusion contribution to the current, rather than as a finite conductivity due to unintentional doping. However, the experimental currents show even stronger thickness dependence. Considering that the thickness dependence is the same for both the linear and quadratic regions, it is evident that the effective charge-carrier mobility must be thickness dependent. Such a thickness dependence of the effective charge-carrier mobility has been observed earlier for asymmetric MEH-PPV hole-only diodes, by analyzing the space-charge-limited drift currents [11]. The explanation for this phenomenon is that the mobility depends on charge-carrier density [12].

We can now apply Eq. (9) to determine the effective charge-carrier mobility from the linear regime of the experimental current-voltage characteristics. The advantage of determining the mobility in the diffusion-dominated regime is that the influence of the electric field is negligible. The mobility is solely influenced by the effective density of diffused carriers from the contacts, p_0. Figure 4(a) shows the effective charge-carrier mobility at 295 and 255 K plotted against layer thickness, where the mobility is determined by fitting Eq. (9) to the linear diffusion regime. In Fig. 4(b) the mobilities are plotted against the effective density p_0, which can be calculated from the layer thickness with Eq. (7). The experimentally obtained mobility has a clear dependence on charge-carrier density, as reported before [12]. This density dependence of the mobility arises from the disordered nature of many organic semiconductors. In the case of an energetically distributed density of states, the carriers first fill the lower-lying states. As the carrier density increases, more hopping states become available, resulting in less energy required for a charge carrier to jump to a neighboring site [13]. The density, electric field, and temperature dependence of the mobility in disordered

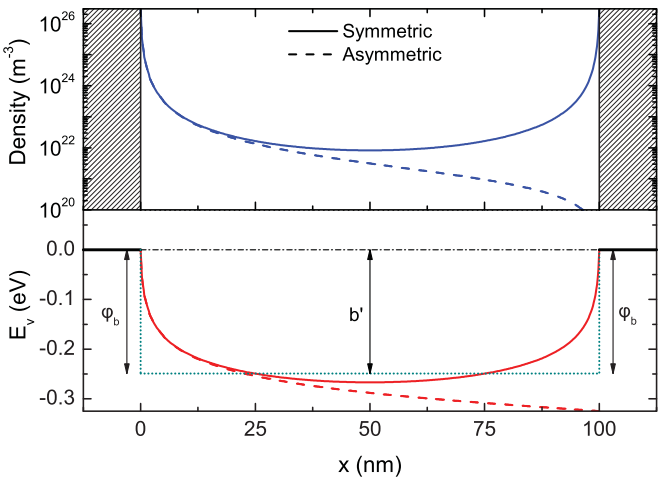

FIG. 3. (Color online) (a) Carrier-density distribution as a function of position in a 100 nm symmetric and asymmetric device. (b) Corresponding valence-band edge, indicating the band-bending parameter b'.

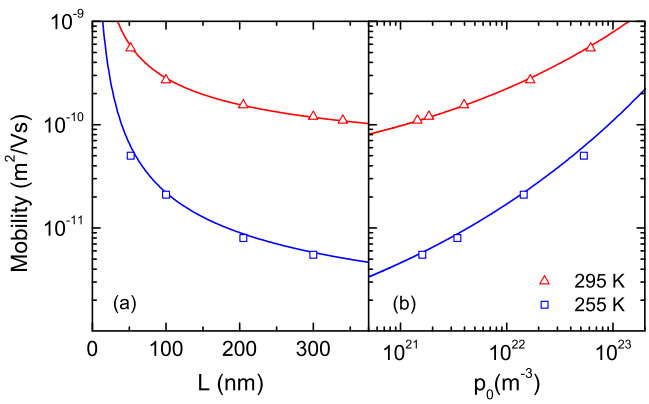

FIG. 4. (Color online) Mobility extracted from the linear regime [Eq. (9)] vs layer thickness (a) and effective carrier density (b) at 295 and 255 K. The solid lines represent the mobility-density relation of the EGDM at zero electric field with the mobility parameters determined by numerical fitting of the J-V characteristics.

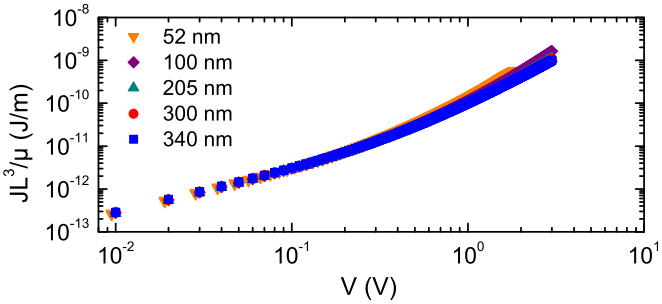

FIG. 5. (Color online) Scaled J-V characteristics for a range of layer thicknesses, confirming the $1/L^3$ scaling of the current in combination with a density-dependent mobility.

semiconductors is well described by the extended Gaussian disorder model (EGDM) [14]. Using a width of the density-of-states distribution σ of 0.145 eV and an average intersite distance of 1.6 nm, the J-V behavior of MEH-PPV hole-only diodes as a function of temperature is well described by numerical simulations.

Figure 4(b) shows that the mobility-density relation that we extracted from the analytic analysis of the Ohmic diffusion current is equivalent to the relation extracted from numerical simulations using the EGDM. Without numerical simulations it is impossible to obtain the density dependence of the mobility at low temperatures from current-voltage measurements on asymmetric organic-semiconductor diodes, since the electric-field dependence of the mobility starts to dominate over the density dependence of the mobility [7]. In the linear regime of a symmetric device, however, field enhancement of the mobility is negligible, so that only density effects need to be taken into account. With the analytical expression for the effective charge concentration and diffusion current the mobility-density relationship can be studied in more detail. Together with the temperature dependence, the density dependence of the mobility can give valuable information on the amount of disorder in organic semiconductors. The validity of the analysis was also confirmed for different classes of conjugated polymers, as indicated in the Supplemental Material [6].

With the mobility known for all layer thicknesses, we can now rescale the current-voltage characteristics by accounting for the density-dependent mobility. In Fig. 5 the data from Fig. 2(a) are replotted by multiplying the current density by L^3/μ. In the linear region the data now collapse onto a single curve for all layer thicknesses. Also in the drift regime the curves are on top of each other, proving that the thickness and mobility dependence are the same for the drift and diffusion regimes. Only at high voltages, an expected small deviation can be seen, which is due to a difference in electric field and space-charge density for different layer thicknesses. We note that the mobility determined for the 100 nm device, as can be seen in Fig. 4(a), is substantially lower than the mobility extracted from the incorrect analysis of the classical space-charge-limited current in Fig. 1. At room temperature, the J-V characteristics appear to be quadratic, which would imply a voltage-independent mobility. However, the influence of the diffusion contribution to the current partially masks the actual field and density dependence of the mobility. Determination of the mobility with the classical standard SCLC analysis can only be performed for fields at which diffusion is negligible. If the mobility depends on carrier density and electric field, the mobility will be overestimated. By taking both drift and diffusion into account, the analysis of charge transport in single-carrier devices can be significantly improved.

In conclusion, Ohmic currents in symmetric organic metal-insulator-metal devices were investigated. It was demonstrated that these currents do not originate from a background carrier density due to unintentional doping, but are due to charge carriers diffusing from the metal contacts into the organic-semiconductor layer. The linear diffusion currents were shown to exhibit the same layer-thickness dependence as the quadratic space-charge-limited drift currents. With the derived analytical expressions for the diffusion current and the effective charge concentration, the mobility and its concentration dependence can be accurately determined from the Ohmic diffusion regime. The advantage is the possibility of determination of the mobility at virtually zero electric field. Analysis of the Ohmic current regime therefore provides a powerful and easy tool to disentangle the effect of charge-carrier density and electric field on the mobility of undoped solids. This will lead to improved insight in the effects of energetic disorder on charge transport.

The authors would like to thank Ilias Katsouras for contributions to this work and Jan Harkema for technical assistance.

[1] N. F. Mott and R. W. Gurney, *Electronic Processes in Ionic Crystals* (Oxford University Press, London, 1940).

[2] P. W. M. Blom, M. J. M. de Jong, and J. J. M. Vleggaar, Appl. Phys. Lett. **68**, 3308 (1996).

[3] P. de Bruyn, A. H. P. van Rest, G. A. H. Wetzelaer, D. M. de Leeuw, and P. W. M. Blom, Phys. Rev. Lett. **111**, 186801 (2013).

[4] M. A. Lampert, Phys. Rev. **103**, 1648 (1956).

[5] M. Kröger, S. Hamwi, J. Meyer, T. Riedl, W. Kowalsky, and A. Kahn, Appl. Phys. Lett. **95**, 123301 (2009).

[6] See Supplemental Material at http://link.aps.org/supplemental/10.1103/PhysRevB.89.241201 for details regarding the symmetric characteristics, band bending, comparison with numerical device simulations, and additional experimental data.

[7] C. Tanase, P. W. M. Blom, and D. M. de Leeuw, Phys. Rev. B **70**, 193202 (2004).

[8] J. G. Simmons, J. Phys. Chem. Solids **32**, 1987 (1971).

[9] R. de Levie and H. Moreira, J. Membr. Biol. **9**, 241 (1972); R. de Levie, N. G. Seidah, and H. Moreira, *ibid.* **10**, 171 (1972).

[10] S. L. M. van Mensfoort and R. Coehoorn, Phys. Rev. B **78**, 085207 (2008).

[11] N. I. Craciun, J. J. Brondijk, and P. W. M. Blom, Phys. Rev. B **77**, 035206 (2008).

[12] C. Tanase, E. J. Meijer, P. W. M. Blom, and D. M. de Leeuw, Phys. Rev. Lett. **91**, 216601 (2003).

[13] M. C. J. M. Vissenberg and M. Matters, Phys. Rev. B **57**, 12964 (1998).

[14] W. F. Pasveer, J. Cottaar, C. Tanase, R. Coehoorn, P. A. Bobbert, P. W. M. Blom, D. M. de Leeuw, and M. A. J. Michels, Phys. Rev. Lett. **94**, 206601 (2005).